Geoderma 189-190 (2012) 574–584

Contents lists available at SciVerse ScienceDirect

Geoderma

journal homepage: www.elsevier.com/locate/geoderma

Strontium isotopes and nutrient sourcing in a semi-arid woodland

Amanda C. Reynolds [a], Jay Quade [b,*], Julio L. Betancourt [c]

[a] Exxon-Mobil Corporation, 4550 Dacoma Street, Houston, TX 77092, USA
[b] Department of Geosciences, University of Arizona, Tucson, AZ 85721, USA
[c] U.S. Geological Survey, 1955 E. 6th St., Tucson, AZ 85719, USA

ARTICLE INFO

Article history:
Received 7 November 2011
Received in revised form 7 June 2012
Accepted 21 June 2012
Available online xxxx

Keywords:
Strontium isotopes
Nutrient cycling
Atmospheric dust
Soil chronosequence
Basalt flows

ABSTRACT

Sr isotopes are widely used as a tracer of Sr and Ca in surficial systems. Basalt flows ranging in age from 3 ka (kiloyears ago) to > 200 ka from El Malpais National Monument (EMNM), New Mexico provide an ideal setting to examine strontium, and hence calcium cycling by plants in a semi-arid woodland. To gauge plant dependence on atmospheric dust versus local weathering products for strontium and calcium, we measured $^{87}Sr/^{86}Sr$ ratios in local bedrock and soils, and compared them to leaf/wood cellulose of four different conifers, a deciduous tree, three shrubs, an annual C_4 grass, and a lichen. Sampling sites varied by parent material (limestone, sandstone, granite, and basalt) and age (Quaternary to Precambrian), providing a wide range in end-member $^{87}Sr/^{86}Sr$ ratios, whereas the target plant species varied in physiognomy, life history, and rooting depth. On non-basalt parent material, the contribution from dust changed with the supply of weatherable Sr-bearing minerals in local bedrock. Soils developed on Paleozoic limestone showed significant bedrock contributions. On basalts, the Sr budget of soils at EMNM is dominated by atmospheric dust on young, 3 ka flows, incorporates a mixture of basalt-dust in 9 ka flows, and is basalt-dominated in 120 ka flows. This is unlike the pattern observed in tropical soils developed on basalt in Hawaii, where basalt weathering dominates the Sr inventory of the youngest soils and aerosols dominate in older, deeply weathered soils. This contrast is mainly due to different water/rock (W/R) ratios: bedrock subjected to high W/R over short periods is quickly (< 10 ka) depleted in Sr (and Ca), except for the ongoing replenishment from aerosols. In arid settings where W/R are lower, soil Sr is still abundantly available first from dust, and increasingly from bedrock even after 120 ka. For plants, $^{87}Sr/^{86}Sr$ variations within and across sites at EMNP showed that evergreen trees varied most in $^{87}Sr/^{86}Sr$ ratios, shrubs were least dependent on eolian input of Sr, and both foliage density and rooting depths influence soil Sr pools.

© 2012 Published by Elsevier B.V.

1. Introduction

The conversion and transfer of rock-derived elements, specifically, calcium (Ca) and strontium (Sr), through soils to plants can be traced using strontium-87/strontium-86 ($^{87}Sr/^{86}Sr$) ratios. Plant Sr and Ca can come either from relatively deep in soils through the slow chemical weathering of local substrates or from shallow soil depths by the alteration of silt-sized, carbonate-rich dust. Although Sr is not itself a plant essential nutrient, it is a common chemical tracer of plant-essential nutrient Ca and exists in all common minerals where Ca is present. Therefore, $^{87}Sr/^{86}Sr$ ratios, which do not significantly fractionate with dissolution, have been used to trace Ca movement from rock or dust to soil water to plants across different climatic, vegetation, and geologic settings (e.g., Chadwick et al., 1999; Vitousek et al., 1999).

We used $^{87}Sr/^{86}Sr$ ratios to evaluate sources and rates of nutrient cycling at El Malpais National Monument (EMNM) in west-central New Mexico, USA (Fig. 1), a semi-arid setting characterized by cold winters, mild summers and bimodal precipitation patterns. This site offers an ideal setting for these kinds of studies. A range of basaltic lava flows and cinder cones (the Zuni-Bandera volcanic field), reminiscent of Hawaiian-style volcanism, erupted over the last 700,000 years in a valley flanked by outcrops of Paleozoic age carbonate rocks, Mesozoic age sandstones, and Precambrian age gneiss (Laughlin et al., 1994). The flows are easily differentiated (Fig. 2) based on very different stages of surface modification and soil development.

The flows and surrounding bedrock are dominated by pinyon-juniper and ponderosa pine woodlands and encompass a wide range of functional plant types with different foliage densities (and thus dust-trapping ability), varied rooting depths, and potentially different strategies of Sr and Ca acquisition. Growing conditions here range from the seemingly impossible – within crevasses in fresh basalt flows and in shallow pools of dust on rock surfaces – to thick, fertile soils. Because the dust and bedrock substrates at EMNM have distinguishable $^{87}Sr/^{86}Sr$ ratios, we can determine the relative contributions

* Corresponding author. Tel.: +1 520 818 8006; fax: +1 520 621 2672.
E-mail address: quadej@email.arizona.edu (J. Quade).

0016-7061/$ – see front matter © 2012 Published by Elsevier B.V.
doi:10.1016/j.geoderma.2012.06.029

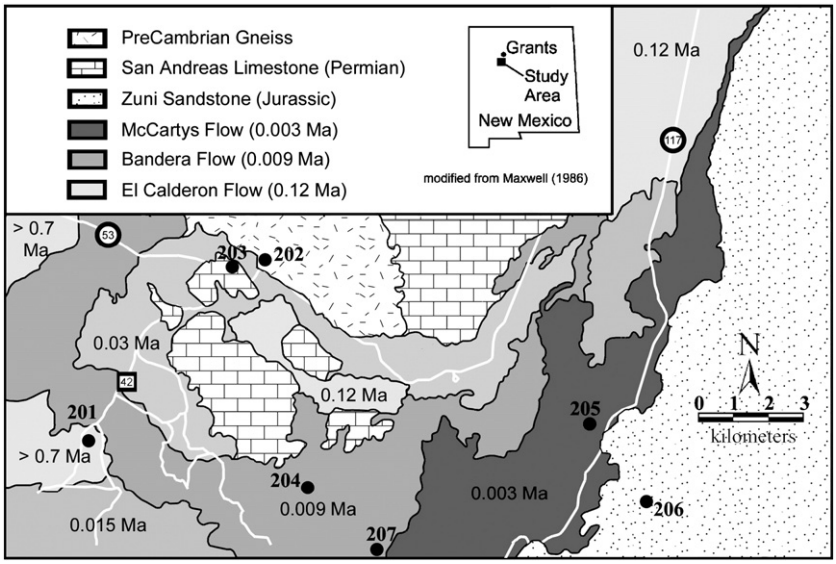

Fig. 1. Generalized geologic map in and around Malpais National Monument with sample sites numbered in bold. Ages of basalt flows indicated in millions of years (Ma). Geology drawn from Maxwell (1986).

of substrate-derived versus dust-derived Sr for different plant species, and compare plant nutrient acquisition patterns across different substrate types and ages.

We measured the $^{87}Sr/^{86}Sr$ ratios in both soils and plants across seven sites that vary by bedrock type (limestone, sandstone, granite, and basalt) and by surface age on 3 ka to 120 ka old basalts and on older non-basalt substrates (Precambrian gneiss and the Mesozoic age Zuni Sandstone and Paleozoic age San Andres Formation) (Table 1). We sampled wood or leaf cellulose from several individuals each for trees (*Pinus ponderosa, Pinus edulis, Juniperus monosperma, Juniperus scopulorum*), shrubs (*Chrysothamus nauseosus, Fallugia paradoxa, Rhus trilobata*), grass (*Bouteloua gracilis*), and lichen (*Xanthoparmelia lineola*) and used an isotopic mixing equation to identify Sr sources. These species exhibit a wide range of life history, growth form and rooting depths (Fig. 3 and Table 2). Typically, more than half of the listed species were represented at each site, allowing for modest replication.

Atmospheric dust contribution to Sr pools was calculated using a simple isotopic mixing equation. Dust $^{87}Sr/^{86}Sr$ ratios at EMNM are dominated by marine carbonates with minor contributions from other bedrock sources (Van der Hoven and Quade, 2002). The relative flux of plant-available Sr from atmospheric and bedrock weathering sources were used to calculate bedrock weathering rates in this semi-arid ecosystem. We compared these rates with those obtained for similar studies conducted in tropical settings at the other end of the climate spectrum (e.g., Chadwick et al., 1999; Kennedy et al., 1998; Stewart et al., 2001; Vitousek et al., 1999).

1.1. Additional background

1.1.1. The role of atmospheric dust and foliage density

Continentally derived dust is an important source of Sr in soil in southwestern United States due to its high carbonate content, high Ca and Sr concentrations, and the susceptibility of carbonate to rapid dissolution compared to silicates. Weathering of limestone and dolostone, and recycled soil caliche provide a relatively stable atmospheric dust source that can locally dominate the Sr inventory in desert soils (Capo and Chadwick, 1999; Van der Hoven and Quade, 2002). In the San Pedro/Nacimiento Mountains near Cuba, New Mexico, the overriding influence of regional atmospheric dust is reflected in conifer $^{87}Sr/^{86}Sr$ ratios, which vary much less than ratios of underlying bedrock, despite growing on three different substrates (granite, limestone, and sandstone) (English et al., 2001). In nearby southern Arizona, Ca and Sr largely derived from dust dominates regional soils and only varies on the rather course scale of ~10^4 km^2 (Naiman et al., 2000).

Several studies have quantified the eolian contribution to soils in the southwestern United States using $^{87}Sr/^{86}Sr$ ratios as a proxy for Ca movement in soils. Using mass balance and $^{87}Sr/^{86}Sr$ ratios on a 2-million-year-old soil in southern New Mexico, Capo and Chadwick (1999) estimate a minimum atmospheric contribution of ~94% to the soil carbonate Ca and 50–70% eolian contribution to the uppermost 25 cm of the soil, suggesting very slow rates of local bedrock weathering. A study of the soil carbonate within EMNM found the $^{87}Sr/^{86}Sr$ ratio of the soil carbonate (=0.7086) and the labile fraction of the A-horizon ($^{87}Sr/^{86}Sr$=0.7075) to be similar to that of the local

Fig. 2. Photographs of typical plant and soil cover on the three main age groups of basalts. From left to right, the McCarty's Flow (3 ka), the Bandera Flow (9 ka), and El Calderón Flow (120 ka).

Table 1
Locality descriptions from El Malpais National Monument, New Mexico.

Site	Bedrock substrate	Lat (N)	Long (W)	Elevation (m)	Age (ka)	Soils
201	El Calderón Flow	34°58.056	108°00.429	2228	120	Silty eolian in depressions Calciorthid Cambic horizon *Stage II carbonate
204	Bandera Flow	34°56.714	108°06.354	2337	9	Semi-continuous rocky bedrock
207		34°56.271	107°54.349	2084		Loamy eolian fill in a some depressions Psamment or Orthent
205	McCarty's Flow	34°50.750	107°55.207	2177	3	Continuous rocky bedrock Minor silt in fractures and Potholes (Orthent) Weak Stage I carbonate
202	Pre-Cambrian gneiss	34°59.021	108°00.725	2254	<10	Rocky alluvial terrace derived from gneiss Fluvent Weak Stage I carbonate
203	San Andres Limestone	35°00.865	108°06.191	2392	~50–100	Alluvial cover on limestone, Calciorthid Stages II–III carbonate
206	Zuni Sandstone	34°43.259	107°55.693	2163	<10	Sandy alluvium derived from Zuni sandstone Psamment Weak Stage I carbonate

*Stages of carbonate from Gile et al. (1966); see text.

atmospheric dust ($^{87}Sr/^{86}Sr = 0.7090$) (Van der Hoven and Quade, 2002), showing that dust is the main source of soil Sr.

In semi-arid ecosystems, a number of factors likely control Sr (and therefore Ca) uptake by plants. Among them, foliar trapping and incorporation of throughfall into the underlying soil appears to be an important source of Sr in plants. Within the Sangre de Cristo Mountains of northern New Mexico, Graustein (1981) and Graustein and Armstrong (1983) demonstrated that 60–80% of the Sr in the trees was derived from canopy throughfall in atmospheric dust and the remaining 20–40% from bedrock weathering. Plant rooting depth is another factor: the deeper the rooting system, the greater the importance of bedrock Sr over eolian Sr added to the top of the soil profile. This factor was not considered in the Graustein studies but is examined here in our research.

1.1.2. The role of soil moisture and rooting depth

Nutrient availability depends in large part on soil moisture because without water plants cannot acquire nutrients, regardless of source. Semi-arid plants use several strategies to both minimize water loss and obtain limited water resources. Such strategies include development of a tap root, possibly to access deeper water (e.g., Breshears et al., 1999) and/or nutrients (e.g., Walvoord et al., 2003) and maximize growth during the winter rainy season. Walter (1973) suggested that woody plants obtain moisture from deeper soil levels than more shallowly rooted herbaceous plants. Breshears et al. (1999) acknowledge, however, that woody plants can be either shallowly or deeply rooted. Moreover, plant root systems can play an active role in soil water variability by passively redistributing water along root systems using soil water potential gradients (Meinzer et al, 2004). In addition, seasonality of rainfall can sharply alter vertical soil moisture profiles (D'Odorico et al., 2000). Plants drawing on summer rains use a shallower nutrient pool than plants that draw upon deeper, winter rains.

Other studies suggest that, although soil moisture plays a role, heterogeneity in the availability of nutrients may be the ultimate control on the rooting habits of plants in semiarid ecosystems (Caldwell et al., 1985; McCulley et al., 2004; Walvoord et al., 2003). McCulley et al. (2004) conclude that deep-rooted plants do not necessarily tap deep water, but instead are scavenging for specific nutrients, namely extractable phosphorus. Further, they suggest that passive uptake of water by these rooting systems and a redistribution of that water and nutrients to shallower levels may be significant. Walvoord et al. (2003) suggest that semi-arid plants can access a large but deep reservoir of bioavailable nitrates. Whatever the causes of variable rooting depths in plants, $^{87}Sr/^{86}Sr$ ratios of plants acquiring their Sr from deep in soils should most reflect local bedrock $^{87}Sr/^{86}Sr$ ratios, even where the canopy is extensive. By contrast, their shallow-rooted counterparts at the same site should exhibit $^{87}Sr/^{86}Sr$ ratios closer to atmospheric dust.

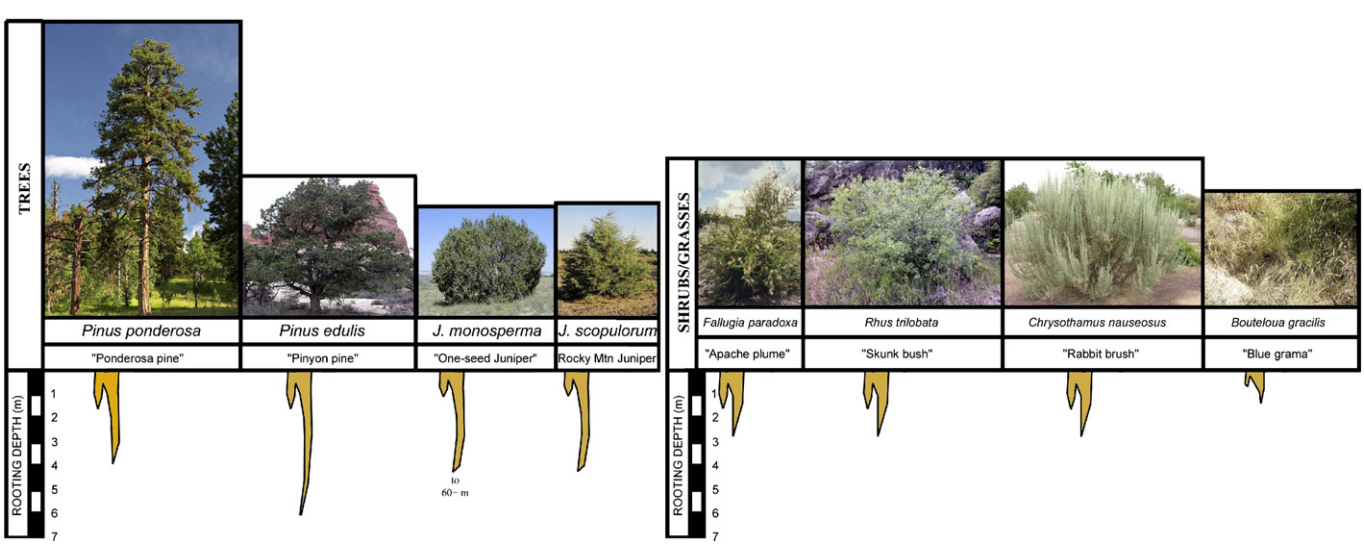

Fig. 3. The main plant species sampled in this study, with typical maximum and minimum rooting depths (refer to Table 2).

Table 2
Typical rooting depths for sampled species taken from the literature.

Species	Common name	Taproot depth (m)	Comments	References
Trees				
Pinus ponderosa	Arizona pine	10–12		1,2
Pinus edulis	Pinyon pine	6		3–6
Juniperus scopularum	Rocky mountain juniper	0.5–4		4,7
Juniperus monosperma	One-seed juniper	60		8
Populus tremuloides	Aspen	NA	Phreatophyte	9
Shrubs				
Fallugia paradoxa	Apache plume	1.4	Endomychorrizal associations	8,10
Rhus trilobata	Skunkbush	NA	Endomychorrizal associations	8
Chrysothamnus nauseosus	Rubber rabbitbrush	2–12	Phreaphyte	11
Grasses				
Bouteloua gracilis	Blue grama	1–2		12

[1] Conkle and Critchfield (1988).
[2] Schubert (1974).
[3] Gottfried (1992).
[4] Foxx and Tierney (1987).
[5] Ronco (1990).
[6] Johnsen (1962).
[7] Canadell et al. (1996).
[8] Williams and Aldon (1976).
[9] Snyder and Williams (2007).
[10] Foxx et al. (1984).
[11] Donovan et al. (1996).
[12] Coupland and Johnson (1965).

2. Environmental setting

EMNM spans from 2100 to 2500 m elevation, with a mean annual precipitation of 420 mm, primarily in summer, and mean monthly maximum/minimum temperatures of 8/−11 °C in January and 31/11 °C in July. Both climate and vegetation varied significantly across the last two glacial–interglacial cycles spanning the age range soil development at EMNM. Mean annual temperatures at EMNM may have been ~5 °C cooler, and winter precipitation was more abundant and regular during the last glacial period than today. Whereas vegetation today is dominated by pinyon-juniper and ponderosa pine woodlands, in the last glacial period the higher elevations of EMNM were probably clad in spruce-fir forest (Betancourt, 1990). Given the longer duration of glacial periods, the study area may have been under boreal or mixed-conifer forests during most of the last million years.

EMNM is part of the Zuni-Bandera volcanic field, dominated by two groups of eruptions. The older flows cover a much larger area, were emplaced at about two times (~600–700 ka and 150 ka), and are difficult to distinguish (Maxwell, 1986). The younger period of eruption includes five major flows, ranging from the El Calderón Flow (120 ka) to the McCarty's Flow (3 ka), which erupted in the western part of the study area and flowed to the northeast (Fig. 1). Laughlin et al. (1994) summarize K–Ar, ^{3}He and ^{14}C dating that constrains the ages of the basalt. The age of a basalt flow provides maximum age constraints for the beginning of soil development. Beneath and surrounding the basalt fields are Precambrian age gneiss flanked by Paleozoic age sandstones and limestones (Yeso and San Andres Formations, respectively) and Mesozoic age sandstones and shales. The Zuni Sandstone, a Jurassic age eolian formation cemented with carbonate, forms a prominent cliff on the eastern edge of the study area (Fig. 1).

A range of soils, most of them previously described in Van der Hoven and Quade (2002) are developed on the different landforms sampled in this study, as summarized in Table 1. On the basalts, surfaces on which plants are growing range from continuous bedrock and a few potholes and crevices filled with eolian dust on the 3 ka McCarty's Flow, to a isolated bedrock knobs and much more continuous eolian cover of up to 1 meter thickness on the 120 ka El Calderón Flows (Van der Hoven and Quade, 2002). Soils on the latter exhibit cambic horizons and isolated carbonate nodules constituting up to Stage II carbonate development (sensu Gile et al., 1966). Soil development on the intermediate 9 ka Bandera Flow is more similar to that of the McCarty's Flow, with isolated thin (<10 cm) patches of eolian silt in depressions.

On non-basaltic substrates, the soils sampled from the pre-Cambrian gneiss and Zuni Sandstone are developed on young (<10 ka) alluvial terraces eroded exclusively from these lithologies (Table 1). The soils are Psamments and Orthents exhibiting the earliest stages of pedogenic carbonate cementation on alluvial clasts, but have no formal diagnostic horizons such as calcic or cambic horizons. By contrast, carbonate continuously coats limestone clasts and partially fills the inter-gravel matrix in the sampled soil on the San Andres Limestone (Stage II–III sensu Gile et al., 1966). Reddened cambic horizons can also be present. This likely denotes ages of 50–100 ka for this soil.

3. Methods

3.1. Field sampling

In June 2002, plant samples were collected from the northern half of EMNM. Ten dominant plant species (*Pinus ponderosa, Pinus edulis, Juniperus monosperma, Juniperus scopulorum, Populus tremuloides, Chrysothamus nauseosus, Fallugia paradoxa, Rhus trilobata, Bouteloua gracilis*, and *Xanthoparmelia lineola*) were sampled. Included are lichen and grass to trees and shrubs that span the range of rooting habits within the monument (Table 2 and Fig. 3). We sampled the innermost (earliest) rings from increment cores taken from *Pinus ponderosa* and *Pinus edulis*, all generally mature trees. When possible, three individuals of each species were sampled for analysis. Sample sites (sites 201–207) were selected to span the seven major rock types/exposure ages of the monument. Sites 204 and 207 both are on Bandera Flow (9 ka) but site 204 is from the middle of the flow and site 207 from its eastern edge. These sites were chosen to test variation in atmospheric dust inputs on the margins of basalt flows bordered by Zuni Sandstone (Fig. 1). Shrub and grass species were sampled from tree intercanopy locations. In June 2006, we took soil samples from the A and B Horizons in hand-dug soil pits in 5-cm increments, typically from the upper 30–50 cm, both from canopy and intercanopy soil profiles in order to measure exchangeable ^{87}Sr/^{86}Sr ratios (and, hence, shallow soil water ^{87}Sr/^{86}Sr).

3.2. Laboratory methods

The outermost 1–2 mm of the tree core's surface was physically removed and discarded to prevent contamination due to handling or storage. For most other species (*Juniperus monosperma, Juniperus scopulorum, Chrysothamus nauseosus, Fallugia paradoxa, Rhus trilobata*) woody material collected from branches and bark was removed before processing. With the grass *Bouteloua gracilis*, samples were sonicated in ultrapure 18 mΩ water and dried before proceeding. A total of 60 to 100 mg of wood (100–200 mg for *B. gracilis*) was then cut into 1–2 mm^3 pieces and placed in an acid-cleaned Vycor tube. The typical sample spanned several years, thus minimizing annual variations in Sr. Samples were combusted between 750 and 850 °C for 12–18 h until all organic matter was ashed. Samples were then transported to a clean lab for wet chemical processing. The remaining inorganic ash was dissolved in distilled 6 M HCl, transferred to a Teflon vial, and, in some samples, an ^{84}Sr tracer was added to allow determination of Sr concentration. The ^{87}Sr/^{86}Sr ratios derived from the plant ash will herein be referred to as ^{87}Sr/^{86}Sr$_{plant}$. We leached dust and soil samples from

Table 3
$^{87}Sr/^{86}Sr$ ratios of plants, bedrock, and dust from basalt flows.

Corrected Class	Species*	Sample^	$^{87}sr/^{86}sr$	2σ	[Sr]	% rock min.	% rock max.
McCarty's Flow (205)							
Trees	Pipo	A	0.707614	54	4.8	57	72
Trees	Pied	C	0.708092	123	6.3	37	60
Trees	Jusc	A	0.707872	24	21.1	47	66
Trees	Jusc	B	0.708029	21	18.5	40	62
Trees	Jumo	A	0.707862	37		47	66
Trees	Jumo	A	0.706764	48	19.4	51	68
Trees	Jumo	B	0.706582	51	8	8	45
Trees	Jumo	B	0.706575	37	7.7	9	45
Shrubs	Fapa	A	0.707840	35		48	67
Shrubs	Fapa	B	0.708068	34		38	61
Shrubs	Fapa	C	0.707706	25	7.4	53	70
Shrubs	Rhtr	B	0.707721	23		53	69
Shrubs	Rhtr	C	0.707890	25	12.6	46	65
Shrubs	Chna	A	0.707809	25	6.6	49	67
Shrubs	Chna	A	0.707891	38	9.6	46	65
Shrubs	Chna	B	0.707775	38	5.8	51	68
Shrubs	Chna	C	0.707828	55	9.7	48	67
Other	Bogr	B	0.708296	67	6.5	26	54
Other	Bogr	C	0.708353	33	3.4	23	52
Rock[1]	Max.		0.7060		293		
Rock[1]	Min.		0.7059				
Soil (A-horizon)[2]			0.7082			31	57
Dust[3]	Max.		0.7096		610		
Dust[3]	Min.		0.7087				
Bandera Flow (204 and 207)							
Trees	Pipo	A	0.706354	54		64	79
Trees	Pipo	B	0.708079	69		22	48
Trees	Pipo	C	0.706432	30	5.3	63	78
Trees	Pipo	C	0.707906	27		28	52
Trees	Pied	A	0.707988	30	4.9	25	50
Trees	Pied	B	0.707766	67	4.2	32	55
Trees	Pied	C	0.706272	31	6.8	65	81
Trees	Jusc	A	0.706809	27	13	55	72
Trees	Jusc	B	0.706351	31	17.3	64	79
Trees	Jusc	B	0.706360	28		64	79
Trees	Jusc	E	0.706643	29		58	75
Trees	Jusc	C	0.706268	113	14.1	65	81
Trees	Jumo	C	0.707619	27	17.9	36	58
Shrubs	Fapa	A	0.706014	30	7.8	70	84
Shrubs	Fapa	A	0.706063	217		69	83
Shrubs	Fapa	B	0.706276	79	8.9	65	81
Shrubs	Fapa	B	0.706280	28	9.2	65	80
Shrubs	Fapa	C	0.706192	28	14.1	67	82
Shrubs	Fapa	C	0.706192	34	14.1	67	82
Shrubs	Rhtr	A	0.706449	29	44.8	62	78
Shrubs	Rhtr	B	0.706236	27	37.5	66	81
Shrubs	Rhtr	G	0.706257	24		66	81
Shrubs	Rhtr	C	0.706283	32	31.4	65	80
Shrubs	Rhtr	C	0.706346	28		64	80
Shrubs	Chna	A	0.706259	30	10.7	66	81
Shrubs	Chna	B	0.706259	27	15	66	81
Shrubs	Chna	C	0.706206	37		67	81
Shrubs	Chna	C	0.706292	30	11.8	65	80
Other	Bogr	B	0.706805	40	7.3	55	73
Other	Xali	A	0.707767	24	34.5	32	55
Other	Potr	A	0.707071	24	7.8	49	68
Other	Potr	B	0.706655	28	9.2	58	75
Other	Potr	B	0.706579	28	93.5	60	76
Other	Potr	B	0.706228	25	42.9	66	81
Other	Pipo (e)	B	0.707208	30		46	66
Other	Pied (e)	A	0.706840	27		54	72
Other	Pied (e)	B	0.707053	20	5.9	50	68
Other	Pied (e)	C	0.707131	24	5.6	48	67
Other	Pipo (o)	A	0.706394	26		63	79
Rock[1]	Max.		0.7046		293		
Rock[1]	Min.		0.7036				
Soil (A-horizon)[2]	Max.		0.7076			36	58
Soil (A-horizon)[2]	Min		0.7066			59	76
Dust[4]	Max.		0.7096		610		
Dust[4]	Min.		0.7087				
	Pothole (w)		0.7071	42			

Table 3 (*continued*)

Corrected Class	Species*	Sample^	$^{87}sr/^{86}sr$	2σ	[Sr]	% rock min.	% rock max.
El Calderón Flow (site 201)							
Trees	Pipo	A	0.705936	14	5.1	89	98
Trees	Pipo	C	0.705539	11	8.1	95	103
Trees	Pied	B	0.705634	28	2.6	94	102
Trees	Pied	C	0.705635	28	2.5	94	102
Trees	Jumo	B	0.705529	35		95	103
Trees	Jumo	C	0.706219	28	29.8	84	94
Shrubs	Fapa	A	0.705425	25	16.1	97	105
Shrubs	Fapa	B	0.705248	25	15.9	99	106
Shrubs	Fapa	C	0.705437	27	15.9	97	104
Shrubs	Rhtr	B	0.704911	41		104	110
Shrubs	Rhtr	C	0.705278	28		99	106
Shrubs	Chna	A	0.706035	37		87	97
Shrubs	Chna	B	0.705492	35		96	104
Shrubs	Chna	B	0.705532	21	14.7	95	103
Other	Bogr	A	0.707384	78	7.2	56	74
Rock[1]		Max.	0.7058		293		
Rock[1]		Min.	0.7052			−166	−40
Soil (A-horizon)[2]		Max.	0.7102			58	76
Soil (A-horizon)[2]		Min	0.7073		610		
Dust[4]		Max.	0.7096				
Dust[4]		Min.	0.7087				

*Plant species abbreviations from the first two letters of genus and species of the plants listed in Table 2 (e.g., Pipo = Pinus ponderosa).
^Each letter denotes individual specimens from a site.
[1]Whole rock ratios (Van der Hoven and Quade, 2002).
[2]A horizon $^{87}Sr/^{86}Sr$ ratios (Van der Hoven and Quade, 2002).
[3]Local dust end-member (this study), used in place of regional end-member when regional dust end-member cannot explain $^{87}Sr/^{86}Sr$ plant ratios.
[4]Regional dust range (Van der Hoven and Quade, 2002; Capo and Chadwick, 1999).

the upper 20–40 cm of soil with 0.1 M NH_4-acetate with a pH 8 in accordance with Jackson (1956) to isolate plant-available elements, herein referred to as the exchangeable fraction ($^{87}Sr/^{86}Sr_{exch.}$). The supernatant was collected and analyzed.

All samples were dried down on a hotplate, redissolved in 3.5 M HNO_3, and run through Eichrom Sr-specific resin columns to isolate the Sr from the sample. Samples were analyzed for $^{87}Sr/^{86}Sr$ and Sr concentration on a thermal ionization mass spectrometer (TIMS) at the University of Arizona. NBS-987 standards were analyzed repeatedly, yielding an $^{87}Sr/^{86}Sr$ ratio of 0.710268 ± 0.00004 ($n = 24$). We measured the $^{87}Sr/^{86}Sr$ ratios on 138 cellulose ($^{87}Sr/^{86}Sr_{plant}$) and 45 soil samples ($^{87}Sr/^{86}Sr_{exch.}$). Bedrock (whole rock) and dust (labile fraction, 1 M acetic acid leachate) end-member ratios are taken from previously published data for EMNM (Van der Hoven and Quade, 2002).

3.3. Bedrock versus atmospheric dust end members

We can estimate proportional inputs of dust versus bedrock Sr within EMNM by comparing the end-member $^{87}Sr/^{86}Sr$ ratios of the exchangeable fraction of local dust ($^{87}Sr/^{86}Sr_{dust}$) and of local bedrock whole-rock ratios ($^{87}Sr/^{86}Sr_{WR}$) (Van der Hoven and Quade, 2002) to $^{87}Sr/^{86}Sr_{plant}$ ratios. The whole-rock $^{87}Sr/^{86}Sr$ ratios of each basalt (Van der Hoven and Quade, 2002) differ through time due to variation in the magma sources. The El Calderón ($^{87}Sr/^{86}Sr_{WR} = 0.7052–0.7058$), Bandera ($^{87}Sr/^{86}Sr_{WR} = 0.7036–0.7046$), and McCarty's ($^{87}Sr/^{86}Sr_{WR} = 0.7059–0.7060$) basalts all display relatively narrow isotopic ranges (Van der Hoven and Quade, 2002). The marine San Andres Limestone ($^{87}Sr/^{86}Sr_{WR} = 0.7077$) is also isotopically homogenous. In contrast, the Zuni Sandstone ($^{87}Sr/^{86}Sr_{WR} = 0.7090–0.7099$) and especially Precambrian gneiss ($^{87}Sr/^{86}Sr_{WR} = 0.8043–0.8644$) are isotopically heterogeneous.

The range of $^{87}Sr/^{86}Sr_{dust}$ ratios at EMNM is 0.7087–0.7096 (Van der Hoven and Quade, 2002). This range is comparable to the range of $^{87}Sr/^{86}Sr$ ratios (labile fraction) in dust measured at Las Cruces, New Mexico (0.7087–0.7093; Capo et al., 1998) and very likely represents the typical background ratio of fine-grained dust for the entire region. Less certain

is the range of compositional variation of coarser dust on a local scale (10^2 km or less). Some sites are within a kilometer of a bedrock transition (Fig. 1). $^{87}Sr/^{86}Sr$ ratios of the exchangeable fraction of A-horizons obtained by Van der Hoven and Quade (2002) and by us can serve as proxies for possible local variation in the dust end member.

4. Results

4.1. Basalt weathering

The $^{87}Sr/^{86}Sr_{plant}$ of plants growing on basalt display relatively narrow isotopic ranges (typically ±0.002) and fall between $^{87}Sr/^{86}Sr_{dust}$ and $^{87}Sr/^{86}Sr_{WR}$ of underlying basalt (Table 3). In general, $^{87}Sr/^{86}Sr_{plant}$ ratios are more like $^{87}Sr/^{86}Sr_{WR}$ of local basalt and less like $^{87}Sr/^{86}Sr_{dust}$ as the age of the basalt flow increases (Table 3). Differences in the $^{87}Sr/^{86}Sr_{plant}$ ratios among the El Calderón (120 ka), Bandera (9 ka), and McCarty's (3 ka) flows are statistically significant and distinct from each other (Fig. 4).

To calculate percentage bedrock contributions to plants, the two-end member isotopic mixing equation (Eq. (1)) was applied to each site using $^{87}Sr/^{86}Sr_{dust}$ and $^{87}Sr/^{86}Sr_{WR}$ end-members [$^{87}Sr/^{86}Sr_{WR}$ taken from Van der Hoven and Quade (2002) and listed in Table 3].

$$\%\text{rock} = 100 * \left[\frac{\left(R_{\text{plant}} - R_{\text{dust}}\right)}{\left(R_{\text{WR}} - R_{\text{dust}}\right)}\right] \quad (1)$$

where $R = {}^{87}Sr/^{86}Sr$.

Using this equation, the Sr in local plants is calculated to be 10–60% bedrock derived on the McCarty's Flow, 40–60% bedrock-derived on the Bandera Flow, and >90% bedrock-derived at the El Calderón Flow (Fig. 5). At the El Calderón site, only *B. gracilis*, a grass, shows a significant eolian input (56% bedrock). At all three basalt sites, $^{87}Sr/^{86}Sr_{plant}$ ratios (Fig. 5) tend to cluster by species and growth form. For example, at the Bandera Site, the site with the largest data set, shrub species with comparable rooting depths have similar $^{87}Sr/^{86}Sr$ ratios (mean $^{87}Sr/^{86}Sr_{plant} = 0.7062 \pm 0.0001$ 1σ, $n = 15$). At the same site, $^{87}Sr/^{86}Sr$ ratios of trees tend to have slightly higher ratios and standard deviations (mean $^{87}Sr/^{86}Sr_{plant} = 0.7070 \pm 0.0007$ 1σ, $n = 13$) compared to shrubs. The grass and lichen tend to have the ratios closest to $^{87}Sr/^{86}Sr_{dust}$ (mean $^{87}Sr/^{86}Sr_{plant} = 0.7073 \pm 0.0007$, $n = 2$).

4.2. The soil $^{87}Sr/^{86}Sr$ exchangeable fraction

The $^{87}Sr/^{86}Sr_{exch}$ ratios of the upper (~30 cm) of soil horizons (Table 4) on the McCarty's, Bandera, and El Calderón Flows show a similar pattern to that of the $^{87}Sr/^{86}Sr_{plant}$. $^{87}Sr/^{86}Sr_{exch.}$ ratios of soil on younger basalt flows tend to fall closer to the $^{87}Sr/^{86}Sr_{dust}$ than those on older basalt flows. We can calculate the fractional contributions of dust and local bedrock to exchangeable soil Sr by substituting $^{87}Sr/^{86}Sr_{exch.}$ for $^{87}Sr/^{86}Sr_{plant}$ in Eq. (1). For example, at the El Calderón site, we calculate an eolian contribution of around 20–30% based on the $^{87}Sr/^{86}Sr_{exch.}$ ratios for both open- and closed-canopy soil profiles, with 10–20% more eolian input in the upper 10 cm in the open canopy site. For an open-canopy Bandera soil, the $^{87}Sr/^{86}Sr_{exch.}$ is approximately 75% eolian. In soil on the McCarty's flow, our youngest flow, the dust contribution to $^{87}Sr/^{86}Sr_{exch}$ increases to 80–90%.

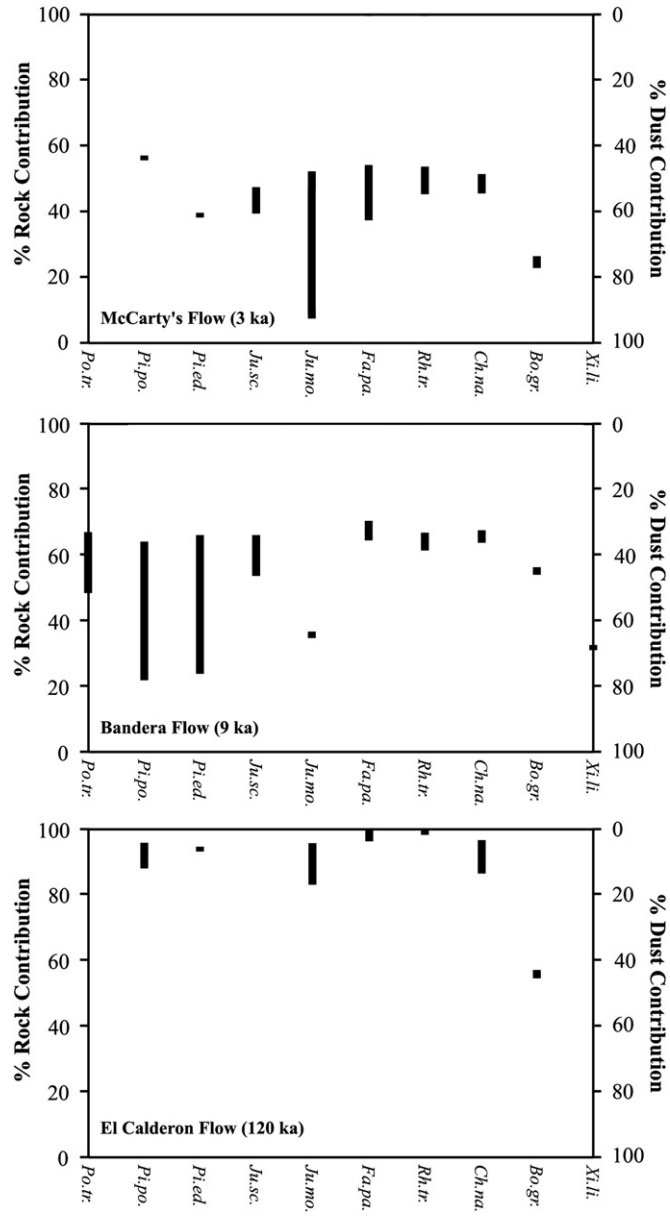

Fig. 5. Maximum estimates of percentage bedrock (left) and dust (right) contribution to plants growing on basaltic parent material. Plant species abbreviations on horizontal axis are from the first two letters of genus and species.

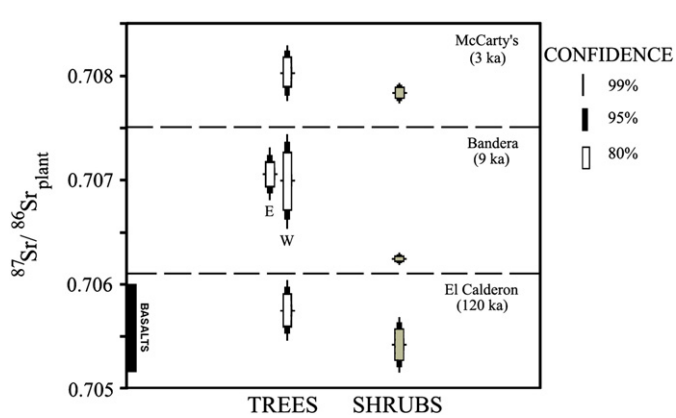

Fig. 4. Bullet graph of $^{87}Sr/^{86}Sr$ ratios of plants (open boxes) on three different basalt flows (ages indicated). For the Bandera Flow, both sites 205 (W) and 207 (E) are plotted. Range of $^{87}Sr/^{86}Sr$ ratios of underlying basalts shown for comparison in black.

4.3. Non-basalt parent material

$^{87}Sr/^{86}Sr_{plant}$ ratios on non-basalt parent materials, especially at sites underlain by Precambrian gneiss and San Andres Limestone, display more isotopic variation (±0.0008–0.003, 1σ) within and among species than seen in the $^{87}Sr/^{86}Sr_{plant}$ on the basalt flows. Local

Table 4
$^{87}Sr/^{86}Sr$ ratios of exchangeable Sr under open- and closed-canopy.

Canopy	Sample depth (cm)	$^{87}Sr/^{86}Sr_{exch}$^	2σ	% rock
El Calderón(201)				
Closed	0–5	0.706288	25	82
Closed	5–10	0.706276	23	82
Closed	15–20	0.705879	27	90
Closed	20–25	0.705728	23	92
Open	0–5	0.707002	42	66
Open	5–10	0.706954	27	67
Open	15–20	0.706764	27	72
Open	20–25	0.706746	25	72
Open	25–30	0.706706	28	73
Open	30–35	0.706644	30	75
Rock[1]	Max.	0.7058		
Rock[1]	Min.	0.7052		
Soil (A-horizon)[2]	Max.	0.7102		
Soil (A-horizon)[2]	Min.	0.7073		
Pre-Cambrian gneiss (202)				
Closed	0–5	0.712826	29	8
Closed	5–10	0.712914	29	8
Closed	10–15	0.713066	27	8
Closed	15–20	0.713165	27	8
Closed	20–25	0.713023	44	8
Closed	25–30	0.713030	20	8
Closed	30–35	0.713175	30	8
Open	0–5	0.712999	29	8
Open	5–10	0.713213	27	8
Open	15–20	0.713085	24	8
Rock[1]	Max.	0.8043		
Rock[1]	Min.	0.8644		
San Andres Limestone (203)				
Closed	5–10	0.708604	48	10
Closed	5–10	0.708744	91	−4
Closed	10–15	0.708703	24	0
Closed	15–20	0.708720	65	−2
Closed	20–25	0.708807	26	−11
Open	10–15	0.708786	27	−9
Rock[1]		0.7077		
Dust[3]		0.7148		
Bandera Flow (204)				
Open	5–10	0.708070	30	23
Open	20–25	0.708008	28	25
Open	25–30	0.708015	24	24
Open	30–35	0.708012	25	25
Rock[1]	Max.	0.7046		
Rock[1]	Min.	0.7036		
Soil (A-horizon)[2]	Max.	0.7076		
Soil (A-horizon)[2]	Min.	0.7066		
Dust[3]	Pothole	0.707051		
McCarty's Flow (205)				
Closed	0–5	0.708537	60	11
Closed	15–20	0.708564	26	10
Closed	25–30	0.708439	24	18
Open	30–35	0.708365	23	22
Rock[1]	Max.	0.7060		
Rock[1]	Min.	0.7059		
Soil (A)[2]	Max.	0.7082		
Zuni sandstone (206)				
Closed	35–40	0.708339	23	−421
Closed	40–45	0.708291	27	−436
Open	0–5	0.708552	33	−349
Open	5–10	0.708487	111	−371
Open	10–15	0.708555	77	−348
Open	15–20	0.708519	40	−361
Open	20–25	0.708713	26	−296
Open	25–30	0.708361	24	−413
Open	40–45	0.708277	24	−441
Open	45–50	0.708308	21	−431
Dust[4]	Max.	0.7096		
Dust[4]	Min.	0.7087		

[1–3]Superscript references same as in Table 3.
^ Dust and soil samples from the upper 20–40 cm of soil leached with 0.1 M NH_4-acetate with a pH 8 in accordance with Jackson (1956).

variation in the $^{87}Sr/^{86}Sr_{dust}$ ratio could be one source of this variation. Nonetheless, clear trends can still be observed within the dataset that track local bedrock lithology. Calculated percentage bedrock contribution to the plant Sr pool for these non-basalt flows (Fig. 6) spans a broad range of ratios (Table 5), largely tracking local lithology.

For the Precambrian gneiss (site 201), $^{87}Sr/^{86}Sr_{plant}$ ratios (Table 5) fall between the dust and substrate end member ratios ($^{87}Sr/^{86}Sr_{WR}$ = 0.8644 and $^{87}Sr/^{86}Sr_{dust}$ = 0.7087), but tend to fall much closer (10–20% bedrock-derived) to the dust end-member (Table 5). The soil $^{87}Sr/^{86}Sr_{exch.}$ at this site (Table 4) is comparable to $^{87}Sr/^{86}Sr_{plant}$ ratios with $^{87}Sr/^{86}Sr_{exch.}$ratios from 0.7128 to 0.7132 (open and closed canopy, respectively).

In sharp contrast, $^{87}Sr/^{86}Sr_{plant}$ ratios at the San Andres Limestone site are dominated by bedrock. For both the San Andres Limestone and Zuni Sandstone sites, lichen $^{87}Sr/^{86}Sr_{plant}$ ratios and pothole $^{87}Sr/^{86}Sr_{dust}$ ratios suggest more locally derived dust sources at these sites, and we adjusted the $^{87}Sr/^{86}Sr_{dust}$ end-members accordingly (Table 5). In our mixing calculations for the San Andreas site we

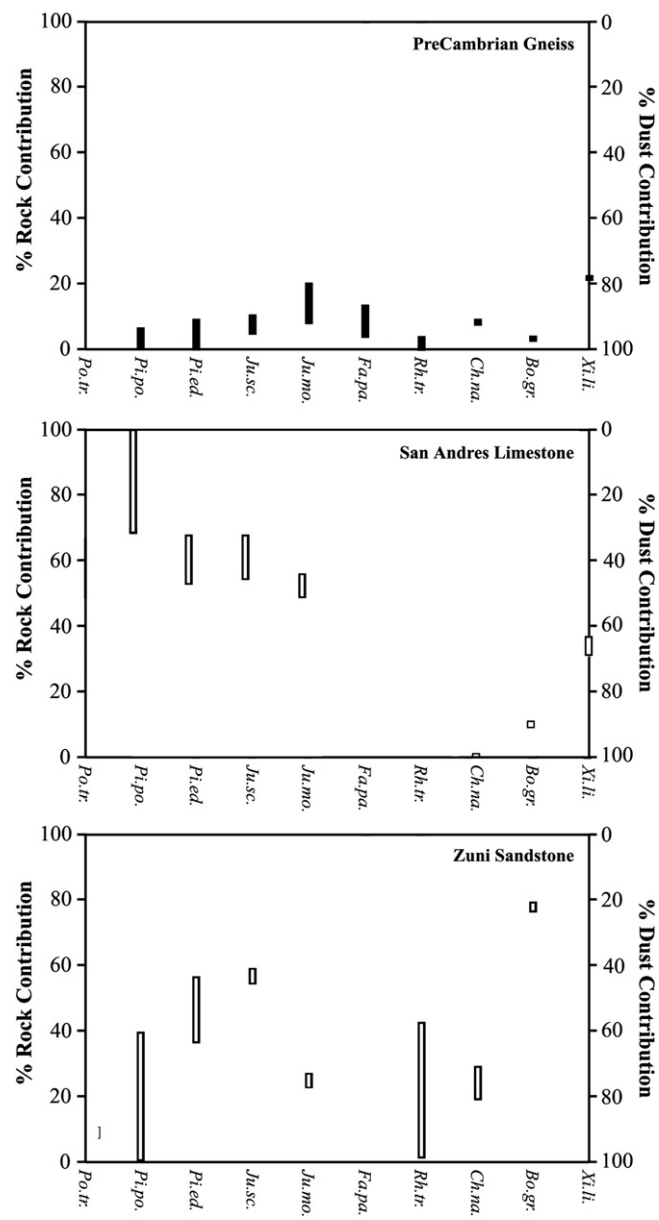

Fig. 6. Maximum estimates of percentage bedrock (left) and dust (right) contribution to plants growing on non-basaltic parent material. Plant species abbreviations on horizontal axis are from the first two letters of genus and species.

Table 5
$^{87}Sr/^{86}Sr$ ratios of plants, bedrock, and dust from non-basalt parent materials.

Corrected								
Class	Species*	Sample^	$^{87}Sr/^{86}Sr$	2σ	[Sr]	% rock min.	% rock max.	% rock corr
Pre-Cambrian gneiss (202)								
trees	Pipo	B	0.711751	11	6.7	6	7	
trees	Pipo	C	0.707882	13	5.8	−2	−6	
Trees	Pied	A	0.707371	30	4.2	−3	−8	
Trees	Pied	B	0.712236	30	4	7	8	
Trees	Pied	C	0.713474	78		9	12	
Trees	Jusc	A	0.711516	24	14.6	5	6	
Trees	Jusc	B	0.711735	26	16.8	5	6	
Trees	Jusc	C	0.714235	29		10	14	
Trees	Jumo	A	0.720308	27		20	28	
Trees	Jumo	A	0.720277	24		20	28	
Trees	Jumo	B	0.713080	33	19.1	8	10	
Trees	Jumo	C	0.714816	37	15.3	11	15	
Shrubs	Fapa	B	0.711209	27		5	5	
Shrubs	Fapa	A	0.715935	33	20.5	13	18	
Shrubs	Fapa	A	0.714416	30		10	14	
Shrubs	Fapa	B	0.711042	28		4	5	
Shrubs	Fapa	B	0.711212	27	14.1	5	5	
Shrubs	Fapa	C	0.715462	49		12	17	
Shrubs	Fapa	C	0.715535	31	8.8	12	17	
Shrubs	Rhtr	B	0.710391	36		3	3	
Shrubs	Rhtr	C	0.708471	98		0	−4	
Shrubs	Rhtr	C	0.708897	28	15.1	0	−2	
Shrubs	Chna	A	0.713184	54	13.2	8	11	
Other	Bogr	B	0.710333	305		3	2	
Other	Xali	A	0.721910	103		22	31	
Other	Pied needles	A	0.713474	78		9	12	
Rock[1]	Max.		0.8043		200			
Rock[1]	Min.		0.8644					
Dust[3]	Max.		0.7096		610			
Dust[3]	Min.		0.7087					
Zuni Sandstone (206)								
Trees	Pipo	A	0.708368	14	6.2	−411	−111	30
Trees	Pipo	B	0.707546	14	3.3	−685	−385	−7
Trees	Pipo	C	0.708556	11	6.2	−348	−48	39
Trees	Pied	A	0.708508	28	5.5	−364	−64	37
Trees	Pied	B	0.708930	26		−223	77	56
Trees	Pied	C	0.708895	28	8.3	−235	65	54
Trees	Jusc	A	0.708914	30	24.9	−229	71	55
Trees	Jusc	B	0.708986	24	26.2	−205	95	58
Trees	Jusc	B	0.708930	26		−223	77	56
Trees	Jumo	B	0.708225	24	20.4	−458	−258	24
Trees	Jumo	C	0.708274	24	17.9	−442	−142	26
Shrubs	Rhtr	A	0.708632	24	17.4	−323	−23	42
Shrubs	Rhtr	A	0.708559	26	37.5	−347	−47	39
Shrubs	Rhtr	B	0.707763	42	21.1	−612	−312	3
Shrubs	Rhtr	B	0.707740	27	14.3	−620	−320	2
Shrubs	Rhtr	C	0.708560	95	12	−347	−47	39
Shrubs	Chna	A	0.708150	28	9.4	−483	−183	20
Shrubs	Chna	A	0.708347	27	12.7	−418	−118	29
Shrubs	Chna	B	0.708274	25	7.8	−442	−142	26
Other	Bogr	A	0.709408	151	7.3	−64	236	78
Rock[1]	Max.		0.7099		610			
Rock[1]	Min.		0.7090					
Dust[4]	Max.		0.7096		610			
Dust[4]	Min.		0.7087					
Dust[3]	Corr.		0.7077		610			
San Andres Limestone (203)								
Trees	Pipo	A	0.707406	55		129	115	114
Trees	Pipo	B	0.706636	28		206	156	166
Trees	Pipo	B	0.706569	12	3.5	213	160	172
Trees	Pipo	C	0.708596	65		10	53	69
Trees	Pied	C	0.708681	22		2	48	67
Trees	Pied	C	0.709208	56	1.5	−58	17	53
Trees	Jusc	A	0.707784	55	5.1	92	96	96
Trees	Jusc	A	0.708659	58	6	4	50	68
Trees	Jusc	C	0.709185	57	5.5	−48	22	55
Trees	Jusc	C	0.709057	88		−36	29	58
Trees	Jumo	A	0.709310	27		−61	15	53
Trees	Jumo	B	0.709174	25	4.2	−47	22	56
Trees	Jumo	C	0.709491	68	4.1	−79	6	49

Table 5 (*continued*)

Corrected								
Class	Species*	Sample^	$^{87}Sr/^{86}Sr$	2σ	[Sr]	% rock min.	% rock max.	% rock corr
San Andres Limestone (203)								
Shrubs	Chna	B	0.706320	40		238	173	199
Shrubs	Chna	C	0.714786	34	17.6	−609	−273	0
Shrubs	Chna	A	0.707072	51	7.3	163	133	133
Other	Bogr	C	0.710232	278		−153	−33	37
Other	Xali	A	0.710626	33		−193	−54	32
Other	Moss	A	0.713025	36		−432	−180	10
Rock[1]	Max.		0.7077		610			
Dust[4]	Max.		0.7096		610			
Dust[4]	Min.		0.7087					
Dust[3]	Corr.		0.7148		200			

*, ^, [1–4] same as in Table 3.

assumed a higher ratio of 0.7148 for $^{87}Sr/^{86}Sr_{dust}$, the highest ratio displayed by shallow-rooted plants, in this case a *C. nauseosus* (Table 5). Such high ratios probably derive from local dust blown off the nearby (Fig. 1) large expanse of pre-Cambrian gneiss.

$^{87}Sr/^{86}Sr_{plant}$ ratios for the Zuni Sandstone site are highly variable (0.7082–0.7087) but tend to fall between the extremes of plants on Precambrian gneiss and on the San Andreas Limestone (Tables 4, 5). In general, $^{87}Sr/^{86}Sr_{plant}$ ratios at the Zuni Sandstone site fall closer to dust than bedrock, as with the Precambrian gneiss site. For the Zuni Sandstone, the dust $^{87}Sr/^{86}Sr$ end-member has been adjusted to 0.7077, the $^{87}Sr/^{86}Sr$ ratio of the San Andres Limestone and the $^{87}Sr/^{86}Sr_{exch.}$ ratio of a dust sample collected from the nearby pothole in the Bandera Flow (site 207). The lowest $^{87}Sr/^{86}Sr_{plant}$ ratios on the Zuni Sandstone site are found in several *R. trilobata* samples and one *P. ponderosa* individual.

4.4. $^{87}Sr/^{86}Sr$ ratios with growth form, soil depth, and canopy position

$^{87}Sr/^{86}Sr_{plant}$ ratios vary systematically with plant growth form. Mean tree $^{87}Sr/^{86}Sr_{plant}$ ratios are closer to the $^{87}Sr/^{86}Sr_{dust}$ than their shrub counterparts at all sites (Tables 3 and 5) and display a larger range of variation (Figs. 4, 7) than non-trees. Among the trees, *Pinus* and *Juniperus*, the most densely foliated tree species, have $^{87}Sr/^{86}Sr_{plant}$ ratios closest to the $^{87}Sr/^{86}Sr_{dust}$. $^{87}Sr/^{86}Sr_{plant}$ ratios from shrubs are less variable and are closer to $^{87}Sr/^{86}Sr_{WR}$ ratios than their tree and grass counterparts.

$^{87}Sr/^{86}Sr_{exchan.}$ ratios do not vary systematically across the relatively shallow soils depths of 35–50 cm that we sampled. On the

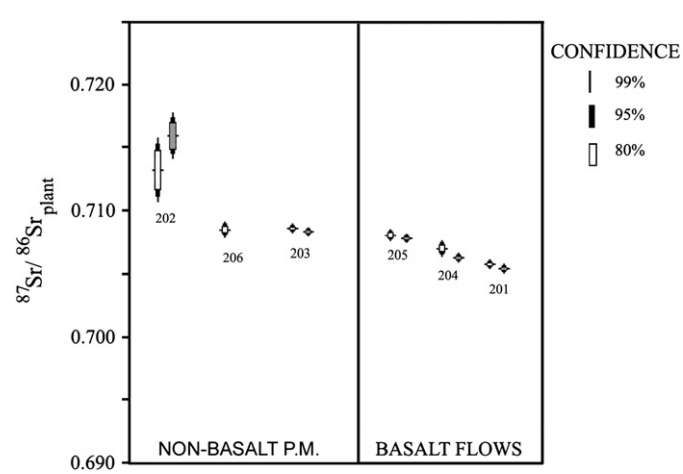

Fig. 7. Bullet graphs of $^{87}Sr/^{86}Sr$ ratios for all tree (white) and shrub (shaded) populations with >3 individuals from sample sites indicated by numbers (see Table 1), on basaltic and non-basaltic parent materials (P.M.).

basaltic soils, especially the well-developed El Calderón (120 ka) profile, $^{87}Sr/^{86}Sr_{exchan.}$decrease systematically with depth (Table 4) between presumed dust ratios at the soil surface to lower ratios that approach local $^{87}Sr/^{86}Sr_{WR}$ ratios at depth. On the non-basaltic soils, patterns in $^{87}Sr/^{86}Sr_{exchan.}$ ratios with soil depth are more complex. For example, they increase with depth on the Precambrian soil under closed but not open canopies. In the Zuni Sandstone soil, depth variation in $^{87}Sr/^{86}Sr_{exchan.}$ ratios is irregular (Table 4).

There also is no clear difference between $^{87}Sr/^{86}Sr_{exchan.}$ ratios under open and closed canopy. El Calderón was the only basaltic site with sufficient soil cover to obtain a large sample. Here open sites have significantly higher $^{87}Sr/^{86}Sr_{exchan.}$ ratios than closed-canopy sites (Table 4). On the non-basaltic sites, there is no systematic difference between open and closed-canopy sites.

5. Discussion

5.1. Growth form and $^{87}Sr/^{86}Sr_{plant}$ ratios

Variable $^{87}Sr/^{86}Sr_{plant}$ ratios over the basalt flow chronosequence can be linked to plant growth form, such as rooting depth and foliage density. Early in the study, we hypothesized that more deeply rooted plants might have bedrock-dominated $^{87}Sr/^{86}Sr_{plant}$ ratios. This hypothesis seems to holds for deep-rooted (down to 2–3 m) shrubs versus shallow-rooted (<1 m) grasses (Table 3). Trees are the most deeply rooted but the most densely foliated plant species, *Pinus* and *Juniperus*, have $^{87}Sr/^{86}Sr_{plant}$ ratios closer to the $^{87}Sr/^{86}Sr_{dust}$. This confirms the finding of Graustein (1981) and Graustein and Armstrong (1983) who demonstrated that throughfall accounts for a significant proportion of most nutrients in mixed-conifer forest. The larger range of variation in tree $^{86}Sr/^{86}Sr_{plant}$ ratios possibly indicates that dense-foliate tree species may have more flexibility in nutrient resource acquisition than their grass and shrub counterparts. This flexibility may allow trees to occupy soils quickly after fire and thus start contributing (by foliar entrapment) to the dust fraction of the soil early in post-fire succession.

The lack of systematic variability in $^{87}Sr/^{86}Sr_{exchan.}$ ratios with soil depth does not necessarily contradict these conclusions. We sampled soil only to 50 cm, far less than the penetration depth of all plants except the grasses. Lack of a clear relationship between $^{87}Sr/^{86}Sr_{exchan.}$and canopy position, however, could mean that trees are not more efficient dust traps that low-stature shrubs and grasses. Alternatively, the short life spans of plants compared to soil could lead to a blurring of potential canopy–soil relationships. For example, trees could take root on sites formally in the open, mixing and overprinting a closed-canopy signature on an open-canopy one.

Several studies have documented the deep-rooting habits of several semi-arid plants that provide access to a more stable groundwater source during drought (Breshears et al., 1999), but also to nutrients such as plant-available phosphorous (Canadell et al., 1996; McCulley et al., 2004) and nitrate (Walvoord et al., 2003). Both tree and shrub species could be utilizing the deeper nutrient pools, but our Sr data suggest that the tree species are less dependent upon them, perhaps because of their ability to utilize throughfall resources. Similarities in the $^{87}Sr/^{86}Sr_{plant}$ ratios between winter-growing *J. monosperma* and summer-growing *P. ponderosa* suggest that phenological differences in plants do not drastically affect nutrient acquisition.

5.2. Sr variation with time and substrate

The $^{87}Sr/^{86}Sr_{plant}$ ratios associated with the basalt flow chronosequence show an increase in bedrock contribution with increasing soil age (Fig. 8). The contribution of basalt weathering to $^{87}Sr/^{86}Sr_{plant}$ is 20–60% on the youngest McCarty's flow (<3 ka), whereas in 120 ka old soil, bedrock dominates plant and exchangeable Sr pools, with $^{87}Sr/^{86}Sr_{plant}$ being 89–100% bedrock-derived.

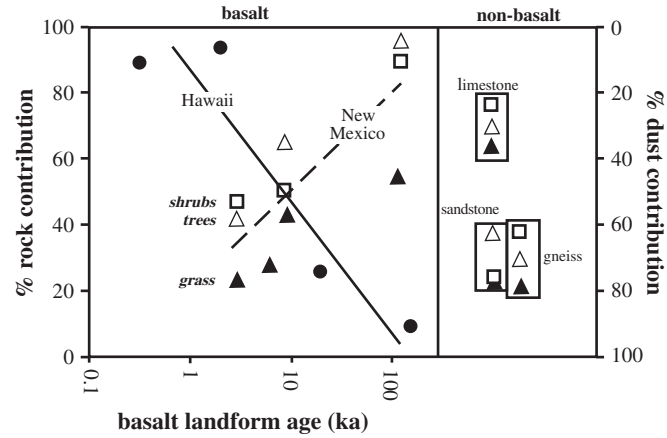

Fig. 8. Tropical versus semi-arid weathering rates. Calculated bedrock and dust contributions to plants shown for soils on basaltic (left) and non-basaltic parent (right). Solid line and solid dots for Hawaii from Kennedy et al. (1998). Dashed line fit to data points (triangles, squares) for New Mexico obtained in this study.

This pattern shows that weathering of dust dominates over bedrock weathering as a source of Sr in the youngest flows, whereas this pattern reverses on the oldest flows. Our data thus indicates that semi-arid soils require many millennia before weathering of silicate bedrock starts to dominate exchangeable soil and plant Sr.

This weathering pattern is the opposite of that observed in basaltic soils from Hawaii (Fig. 8; Kennedy et al., 1998; Stewart et al., 1998). In Hawaii, bedrock weathering provides >90% of Sr to the youngest soils (<2 ka), but <25% of the Sr in soils exceeding 20 ka (Kennedy et al., 1998; Vitousek et al., 1997). Air-borne contributions to the Sr pool increase rapidly as basaltic parent material is depleted by weathering (Vitousek et al., 1999). Moreover, the contribution of atmospheric dust and marine aerosols to soil Sr increases with mean annual precipitation, which varies dramatically across the islands. On a 170-ka basalt flow, for example, Sr at low-rainfall sites (<140 cm/year) is still dominated by weathering of local basalt, whereas dust and marine aerosols contribute most of the Sr in basaltic soils under more humid forests (300 cm/year) (Stewart et al., 2001). Stewart et al. (1998) found that in Hawaii ~25% of the original minerals remain in humid basaltic soils after 170 ka.

Precipitation, temperature, and dust chemical differences probably account for the contrasting behavior of Sr between soils in Hawaii and New Mexico. In semiarid and thinly vegetated New Mexico, the physical and chemical breakdown of basalt is slow, and rates of dust accumulation are thus fast relative to weathering inputs. Furthermore, the dust is fine grained and carbonate rich, and thus weathers quickly, dominating plant-available Sr in the early stages of pedogenesis. Only with the passage of tens of thousands of years does weathering of silicates in basalts start to dominate soil Sr, and this Sr pool remains unexhausted and a dominant even by 120 ka. In tropical and vegetated Hawaii, basalt breaks down quickly and due to elevated precipitation and temperature and rates of dust accumulation are both slower and likely lower in percent carbonate than in New Mexico. For all these reasons, it makes sense that weathering of silicates in basalt dominates exchangeable soil and plant Sr in the earliest stages of pedogenesis. By 150 ka, local basalt substrates are depleted in Sr, and airborne Sr comes to dominate exchangeable Sr in the soil, a stage perhaps never reached in the much drier soils and ecosystems of New Mexico.

Turning to non-basalt soils, we do not have the advantage of age constraints as with the basalt soils, but there are still some very visible effects of parent material weatherability on soil Sr. The $^{87}Sr/^{86}Sr_{plant}$ ratios from soils formed on the Precambrian gneiss show an eolian dominance (>90% eolian) spanning a range of soil morphology from minimal on the slopes to thicker, redder, and clayey soils in more stable landscape positions. From this we conclude that in situ

silicate weathering of the gneiss makes a small contribution to soil Sr, even in older soils. Weathering of dust dominates exchangeable soil and plant Sr at all stages of development. This conclusion is strongly supported by another study of a New Mexico soil developed on quartzofeldspathic alluvium which retained more than 80% of its primary minerals after 2 million years of exposure and yet, showed extremely high eolian influence of the Sr soil pool (>94%) (Capo and Chadwick, 1999; Stewart et al., 1998).

On the other hand, exchangeable soil and plant Sr developed on the Zuni Sandstone and even more so on the San Andres Limestone show a much greater contribution from local rock weathering, 0–50% and 42–98%, respectively, than the case for soils on Precambrian gneiss (20%) (Fig. 8). The reason for this is that carbonate minerals, in this case composing most of the San Andreas Limestone and all of the cements in the Zuni sandstone, weather much more rapidly than silicate minerals, dominating plant-available Sr from the very onset of pedogenesis.

6. Conclusions

$^{87}Sr/^{86}Sr_{plant}$ ratios vary in largely predictable ways according to plant species, rock substrate type, and substrate age. Weathering of dust most strongly influences exchangeable soil and plant Sr on silicate substrates that have undergone relatively little weathering, such as gneiss and young basalt. The contribution of bedrock weathering to exchangeable soil and plant Sr is greatest in soils developed on older basalt flows and carbonate-rich bedrock, such as the San Andreas Limestone.

Rooting depth is the main control on $^{87}Sr/^{86}Sr_{plant}$ ratios in grasses and shrubs. The shallower the rooting depth (grasses), the greater to contribution of dust to $^{87}Sr/^{86}Sr_{plant}$. With trees, dust trapping by dense foliage competes with Sr derived from bedrock by deep roots to determine $^{87}Sr/^{86}Sr_{plant}$. Moreover, trees (*P. ponderosa*, *P. edulis*, and *Juniperus* spp.) display the largest range of $^{87}Sr/^{86}Sr_{plant}$ ratios within a stand, suggesting acquisition of nutrients both from deep bedrock-derived nutrient pools and from throughfall. Closed-canopy versus open-canopy distribution of exchangeable Sr in the shallow soil is not systematic and may be blurred by rapid turnover in plants compared to the longevity of soils.

In the semi-arid settings of western New Mexico, weathering of dust dominates the exchangeable soil and plant Sr on younger basalt flows (<3 ka). The contribution of weathering of local basalt substrate increases with age and dominates over dust weathering by 120 ka. This is the opposite of the pattern observed in basaltic soils in humid Hawaii, where in this wet setting basaltic substrates are quickly depleted of available Sr by weathering and airborne Sr is the main available form after a few thousand years. Differences in rainfall probably account for this contrast.

Acknowledgements

We thank Jon Patchett, Nathan English, and Clark Isachsen for advice on lab protocols. ACR was funded by an NSF-IGERT Fellowship in Archaeometry and an NSF-CATTS Fellowship at the University of Arizona (to ACR). Sampling permits were granted graciously by the Bureau of Land Management and El Malpais National Monument. We thank Thanuj Chandran, Sasha Reed, Steve van der Hoven, and several anonymous reviewers for editorial handling and significant improvement of the manuscript.

References

Betancourt, J.L., 1990. Late Quaternary biogeography of the Colorado Plateau. In: Betancourt, J.L., Van Devender, T.R., Martin, P.S. (Eds.), Packrat middens: The last 40,000 years of biotic change. University of Arizona Press, Tucson, Arizona, pp. 259–292.

Breshears, D.D., Myers, O.B., Johnson, S.R., Meyer, C.W., Martens, S.N., 1999. Differential use of spatially heterogeneous soil moisture by two semiarid woody species: *Pinus edulis* and *Juniperus monosperma*. Journal of Ecology 85, 289–299.

Caldwell, M.M., Eissenstat, D.M., Richards, J.H., Allen, M.F., 1985. Competition for phosphorous: differential uptake from dual-isotope-labelled soil interspaces between shrub and grass. Science 229, 384–386.

Canadell, J., Jackson, R.B., Ehleringer, J.R., Mooney, H.A., Sala, O.E., Schulze, E.D., 1996. Maximum rooting depth of vegetation types at the global scale. Oecologia 108, 583–595.

Capo, R.C., Chadwick, O.A., 1999. Sources of strontium and calcium in desert soil and calcrete. Earth and Planetary Science Letters 170, 61–72.

Capo, R.C., Stewart, B.W., Chadwick, O.A., 1998. Strontium isotopes as tracers of ecosystem processes: theory and methods. Geoderma 82, 197–225.

Chadwick, O.A., Derry, L.A., Vitousek, P.M., Huebert, B.J., Hedin, L.O., 1999. Changing Sources on nutrients during four million years of ecosystem development. Nature 397, 491–497.

Conkle, M.T., Critchfield, W.B. 1988. Genetic variation and hybridization of ponderosa pine. In: Baumgartner, David M.; Lotan, James E., compilers. Ponderosa pine: The species and its management: Symposium proceedings; 1987 September 29 - October 1; Spokane, WA. Pullman, WA: Washington State University, Cooperative Extension, pp. 27–43.

Coupland, R.T., Johnson, R.E., 1965. Rooting characteristics of native grassland species of Saskatchewan. Journal of Ecology 53, 475–507.

D'Odorico, P., Ridolfi, L., Porproto, A., Rodriguez-Iturbe, I., 2000. Preferential states of seasonal soil moisture: the impact of climate fluctuations. Water Resources Research 36, 2209–2219.

Donovan, L.A., Richards, J.H., Muller, M.W., 1996. Water relations and leaf chemistry of *Chrysothamnus nauseosus* ssp. *consimilis* (Asteraceae) and *Sarcobatus vermiculatus* (Chenopodiaceae). American Journal of Botany 83, 1637–1646.

English, N.B., Betancourt, J.L., Dean, J.S., Quade, J., 2001. Strontium isotopes reveal distant sources of architectural timber in Chaco Canyon, New Mexico. Proceedings of the National Academy of Sciences of the United States of America 98, 11891–11896.

Foxx, T.S., Tierney, G.D., 1987. Rooting patterns in the pinyon-juniper woodland. In: Everett, R.L., compiler. Proceedings–pinyon-juniper conference; 1986 January 13–16; Reno, NV. Gen. Tech. Rep. INT-215. Ogden, UT: U.S. Department of Agriculture, Forest Service, Intermountain Research Station, pp. 69–79.

Foxx, T.S., Tierney, G.D., Williams, J.M., 1984. Rooting Depths of Plants to Biological and Environmental Factors. Los Alamos National Laboratory report LA-10254-MS.

Gile, L.H., Peterson, F.F., Grossman, R.B., 1966. Morphological and genetic sequences of carbonate accumulation in desert soils. Soil Science 101, 347–360.

Gottfried, G.J., 1992. Ecology and management of the southwestern pinyon-juniper woodlands. In: Ffolliott, Peter F.; Gottfried, Gerald J.; Bennett, Duane A.; et al., technical coordinators. Ecology and management of oaks and associated woodlands: perspectives in the southwestern United States and northern Mexico: Proceedings; 1992 April 27–30; Sierra Vista, AZ. Gen. Tech. Rep. RM-218. Fort Collins, CO: U.S. Department of Agriculture, Forest Service, Rocky Mountain Forest and Range Experiment Station, pp. 78–86.

Graustein, W.C., 1981. The effects of forest vegetation on solute acquisition and chemical weathering: a study of the Tesuque watersheds near Santa Fe, New Mexico. Ph.D. dissertation. Yale University, 645 pp.

Graustein, W.C., Armstrong, R.L., 1983. The use of strontium-87/strontium-86 ratios to measure atmospheric transport into forested watersheds. Science 219, 289–292.

Jackson, M.L., 1956. Soil chemical analysis-Advanced Course. Mimeo, published by the author. Department of Soil Science. University of Wisconsin, Madison, WI, USA.

Johnsen Jr., T.N., 1962. One-seeded juniper invasion of northern Arizona grasslands. Ecological Monographs 32, 187–207.

Kennedy, M.J., Chadwick, O.A., Vitousek, P.M., Derry, L.A., Hendricks, D.M., 1998. Replacement of weathering with atmospheric sources of base cations during ecosystem development, Hawaiian Islands. Geology 26, 1015–1018.

Laughlin, A.W., Poths, J., Healey, H.A., Reneau, S., WoldeGabriel, G., 1994. Dating of quaternary basalts using the cosmogenic ^{3}He and ^{14}C methods with implications for excess ^{40}Ar. Geology 22, 135–138.

Maxwell, C.H., 1986. Geologic map of El Malpais Lava Field and surrounding areas, Cibola [Valencia] County, New Mexico: U.S. Geological Survey Miscellaneous Investigations Map I-1595, 1 sheet, scale 1:62,500.

McCulley, R.L., Jobbagy, E.G., Pockman, W.T., Jackson, R.B., 2004. Nutrient uptake as a contributing explanation for deep rooting in arid and semi-arid ecosystems. Oecologia 141, 620–628.

Meinzer, F.C., Brooks, J.R., Bucci, S., Goldstein, G., Scholz, F.G., Warren, J.M., 2004. Converging patterns of uptake and hydraulic redistribution of soil water in contrasting woody vegetation types. Tree Physiology 24, 919–928.

Naiman, Z., Quade, J., Patchett, P.J., 2000. Isotopic evidence for eolian recycling of pedogenic carbonate and variations in carbonate dust sources throughout the southwest United States. Geochimica et Cosmochimica Acta 64, 3099–3109.

Ronco Jr., F.P., 1990. *Pinus edulis* Engelm. pinyon. In: Burns, Russell M., Honkala, Barbara H. (Eds.), Silvics of North America. Volume 1. Conifers. : Agricultural Handbook, 654. U.S. Department of Agriculture, Forest Service, Washington, DC, pp. 327–337.

Schubert, G.H., 1974. Silviculture of southwestern ponderosa pine: the status of our knowledge. Res. Pap. RM-123. U.S. Department of Agriculture, Forest Service, Rocky Mountain Forest and Range Experiment Station, Fort Collins, CO. 71 pp.

Snyder, K.A., Williams, D.G., 2007. Root allocation and water uptake patterns in riparian tree saplings: responses to irrigation and defoliation. Forest Ecology and Management 246, 222–231.

Stewart, B.W., Capo, R.C., Chadwick, O.A., 1998. Quantitative strontium isotope models for weathering, pedogenesis, and biogeochemical cycling. Geoderma 82, 173–195.

Stewart, B.W., Capo, R.C., Chadwick, O.A., 2001. Effects of rainfall on weathering rate, base cation provenance, and Sr isotope composition of Hawaiian soils. Geochimica et Cosmochimica Acta 65, 1087–1099.

Van der Hoven, S., Quade, J., 2002. Tracing spatial and temporal variations in the sources of calcium in pedogenic carbonates in a semiarid environment. Geoderma 108, 259–276.
Vitousek, P.M., Chadwick, O.A., Crews, T., Fownes, J., Hendricks, D., Herbert, D., 1997. Soil and ecosystem development across the Hawaiian Islands. GSA Today 7, 1–8.
Vitousek, P.M., Kennedy, M.J., Derry, L.A., Chadwick, O.A., 1999. Weathering versus atmospheric sources of strontium in ecosystems on young volcanic soils. Oecologia 121, 255–259.
Walter, H., 1973. Vegetation of the earth in relation to climate and the eco-physological conditions. Translated from the second German edition by J. Wieser Springer-Verlag, New York.
Walvoord, M.A., Phillips, F.M., Stonestrum, D.A., Evans, R.D., Hartsough, P.C., Newman, B.D., Striegl, R.G., 2003. A reservoir of nitrate beneath desert soils. Science 302, 1021–1024.
Williams, S.E., Aldon, E.F., 1976. Endomycorrhizal (vesicular arbuscular) associations of some arid zone shrubs. The Southwestern Naturalist 20, 437–444.